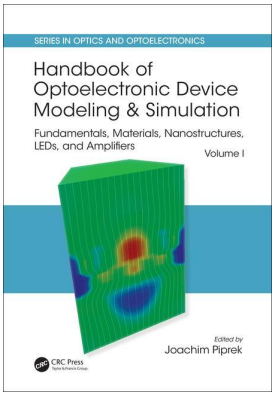

Handbook of Optoelectronic Device Modeling and Simulation Fundamentals, Materials, Nanostructures, LEDs, and Amplifiers

Joachim Piprek

Electron–Photon Interaction

Publication details
https://test.routledgehandbooks.com/doi/10.1201/9781315152301-3
Angela Thränhardt
Published online on: 06 Oct 2017

3

Electron–Photon Interaction

Angela Thränhardt

3.1 Introduction

The devices introduced in this book involve light–matter interaction. Light appears to be a trivial phenomenon known to everyone; however, its mathematical description is quite intricate and has been a major point of discussion in the physics community. Historically, this was manifested in a longstanding dispute on the nature of light, featuring Isaac Newton[†] as the advocate of a corpuscular model and Christiaan Huygens[‡] as the proponent of its wave nature.

Today, more than 300 years later, both perceptions have been reconciled and the description of light in terms of a wave–particle dualism is well established in the physics community. A full quantum-electrodynamic description, relieving the apparent contradiction between wave and particle nature, is often not required, i.e., in many cases, light can be well described as either a wave or a particle. This will be mirrored in this chapter, where both the classical and the quantum perspectives are introduced.

As often stated, the general guideline is that light may be treated as a wave when propagating in vacuum, yet it has to be quantized in the case of the interaction with matter. However, this is not always true, as, e.g., the behavior of light in a waveguide can well be understood in terms of the wave picture. In fact, quantum-optical effects only started to be discussed intensively in the 1950s and 1960s. Their investigation is closely related to the development of the laser and the requirement of solid theoretical foundations in this field. Simply speaking, the corpuscular theory of light states that it is distributed in quantized packages of energy $W = hf = \hbar\omega$, where h is Planck's constant, f is the light frequency, $\hbar = h/(2\pi)$, and ω is the angular frequency $\omega = 2\pi f$. A particle nature is thus attributed to light, where the light particle is known as a photon. The photon may be described quantum mechanically in the framework of second quantization, a formalism in which the light field and other physical field quantities are written as operators. This method was first developed by Paul Dirac[§] in 1927 in analogy to the first quantization where physical quantities

[†] Sir Isaac Newton, English natural philosopher (physicist and mathematician), 1643–1727.
[‡] Christiaan Huygens, Dutch physicist, astronomer, and mathematician, 1629–1695.
[§] Paul Dirac, British physicist, 1902–1984.

such as position and momentum become operators; see Ref. [1]. Further information may be found in textbooks on quantum mechanics.

In this chapter, we consider electron–photon interaction, i.e., light–matter coupling. There are different electron–photon interaction mechanisms, e.g., the photoelectric effect, Compton scattering, and pair production. In the energy range of interest in optoelectronics, the photoelectric effect is the only relevant effect and will thus be treated exclusively.

The chapter briefly introduces the theoretical treatment of electron–photon interaction for different and mostly strongly simplified cases. A large part is devoted to the two-level system in different formalisms. This allows us to concentrate on the differences and commonalities of the various approaches. We look at the two-level system in the Schrödinger and the Heisenberg representation (Section 3.2) and then move on to a solid-state system (Section 3.3). Section 3.4 deals with the quantum-optical treatment of the two-level system, while Section 3.5 is devoted to the treatment of photonic structures.

Before we enter the detailed mathematics of a quantum mechanical system, some basics will be discussed. In any ensemble of atoms or molecules in interaction with an electromagnetic field, there are three processes occurring: spontaneous emission, absorption, and stimulated emission. Although spontaneous emission is quite common in everyday life—e.g., most light sources like light bulbs or light-emitting diodes (LEDs) operate based on spontaneous emission—it is difficult to treat theoretically. The existence of spontaneous emission, however, was already postulated by Albert Einstein in 1916/1917 with his argument based on thermodynamic equilibrium. For a handwaving explanation, consider an ensemble of atoms placed inside a closed cavity whose walls are held at a constant temperature. The walls, furthermore, are assumed to be perfect absorbers and emitters of radiation. After the system has reached thermal equilibrium, the cavity will be filled with the so-called "blackbody radiation" according to the temperature T of the system. The condition of thermal equilibrium then requires that for each transition, the spontaneous emission matches the absorption of blackbody radiation, necessitating the existence of spontaneous emission.

3.2 Two-Level System

3.2.1 Optical Processes in the Two-Level System—A Discussion of the Einstein Coefficients

For a more detailed treatment, we now move to the simplest existing system, the two-level system. It includes one electron that can occupy either one of two nondegenerate states. The two levels of the model may represent, e.g., the highest occupied and lowest unoccupied level in an atom, molecule, or quantum structure. We devote this entire section to the two-level system, including a discussion of the Einstein coefficients as well as calculations in the Schrödinger (Section 3.2.2) and the Heisenberg formalism (Section 3.2.3). In Section 3.4, we again return to the two-level system for a quantum-optical discussion. For an even more detailed treatment of two-level systems, the reader is referred to the book by Allen and Eberly [2].

A schematic of the two-level system is shown in Figure 3.1. The system consists of the ground state, level 1 and one excited state, level 2, with the respective energies ϵ_1 and ϵ_2. One of the levels is occupied by an electron, described by the eigenstates $|1\rangle$ or $|2\rangle$. We consider the interaction with an incident light field with photon density Φ_{ω_0}, where ω_0 refers to the angular light frequency corresponding to the energy difference of the two-level system, $\hbar\omega_0 = \epsilon_2 - \epsilon_1$. Let us now think of an ensemble of identical two-level systems, where the number of electrons in state 1 is N_1 and the number of electrons in state 2 is N_2. The following processes indicated in the schematic may occur in any of them:

1. *Spontaneous emission*, as described earlier, lowering an electron from the excited into the ground state and emitting a photon. The rate of spontaneous emission ρ_{spont} must therefore be proportional to the number of electrons in the excited state

$$\rho_{\text{spont}} = AN_2. \tag{3.1}$$

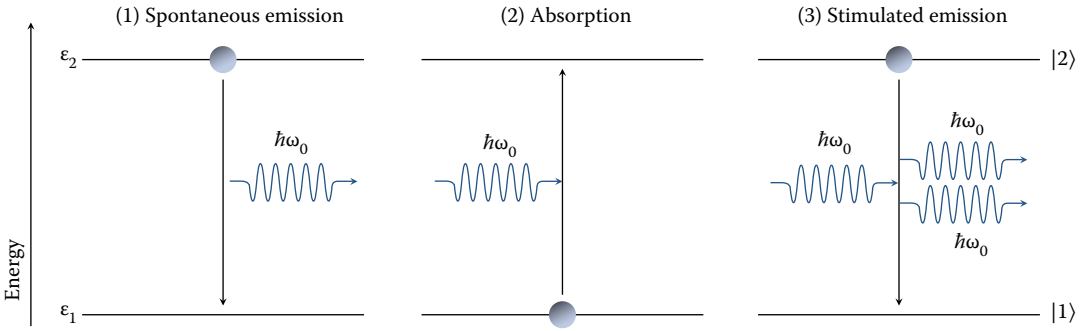

FIGURE 3.1 Relevant electron–photon interaction processes in a two-level system.

2. *Absorption*, raising an electron from the ground state into the excited state by absorbing an existing photon. The rate of absorption ρ_{abs} must be proportional to the number of electrons in the ground state and the photon density at the resonance frequency:

$$\rho_{\text{abs}} = B_{12} N_1 \Phi_{\omega_0}. \tag{3.2}$$

3. *Stimulated emission*, where an electron is stimulated by a photon to emit a second photon and drop to the ground state in consequence. Both photons agree in frequency and phase and travel in the same direction. The rate of stimulated emission ρ_{stim} is proportional to the number of electrons in the excited state and the photon density at resonance

$$\rho_{\text{stim}} = B_{21} N_2 \Phi_{\omega_0}. \tag{3.3}$$

A, B_{12}, and B_{21} are the *Einstein coefficients*, named after Albert Einstein (1879–1955), who first introduced them in 1916; see Ref. [3]. Considering all three processes, we get an expression for the overall rate of change of the occupancies of the two levels:

$$\frac{\mathrm{d}N_1}{\mathrm{d}t} = -\frac{\mathrm{d}N_2}{\mathrm{d}t} = -N_1 B_{12} \Phi_{\omega_0} + N_2 B_{21} \Phi_{\omega_0} + N_2 A. \tag{3.4}$$

Thinking of a thermal equilibrium situation, we demand

$$\frac{\mathrm{d}N_1}{\mathrm{d}t} = \frac{\mathrm{d}N_2}{\mathrm{d}t} = 0, \tag{3.5}$$

which, after substituting Equation 3.4 into 3.5 and making some algebraic conversions, renders

$$\frac{N_2}{N_1} = \frac{B_{12}}{B_{21}\Phi_{\omega_0} + A}. \tag{3.6}$$

On the other hand, thermodynamics tells us that the equilibrium distribution between ground and excited state is governed by the Boltzmann distribution,

$$\frac{N_2}{N_1} = \frac{e^{-\epsilon_2/(k_{\text{B}}T)}}{e^{-\epsilon_1/(k_{\text{B}}T)}} = e^{-\hbar\omega_0/(k_{\text{B}}T)}, \tag{3.7}$$

where k_B is the Boltzmann constant. Equating Equation 3.6 with Equation 3.7 and solving for the photon density Φ_{ω_0} yields

$$\Phi_{\omega_0} = \frac{A}{B_{21}} \frac{1}{\frac{B_{12}}{B_{21}} e^{\hbar\omega_0/(k_B T)} - 1}. \tag{3.8}$$

Now consider Planck's law,

$$\Phi_{\omega_0} = \frac{2\hbar {\omega_0}^3}{\pi c^3} \frac{1}{e^{\hbar\omega_0/(k_B T)} - 1}, \tag{3.9}$$

where c is the velocity of light. Equations 3.8 and 3.9 are very similar in form. A comparison of the two yields

$$B_{12} = B_{21} \equiv B, \tag{3.10}$$

$$A = B \frac{2\hbar {\omega_0}^3}{\pi c^3}. \tag{3.11}$$

Thus, the coefficients of absorption and stimulated emission are equal. This also implies that the relative strength of absorption and stimulated emission is determined exclusively by the occupation of ground and excited state. The coefficient of spontaneous emission, A, is also directly and independently of temperature related to the other two Einstein coefficients.

3.2.2 The Two-Level System in the Schrödinger Picture

We now proceed to a quantum-mechanical treatment of the electron in the two-level system. At this point, we stick to a semiclassical treatment, i.e., a classical treatment of light. As we see, this takes us a long way toward understanding absorption and stimulated emission as well as deriving the optical Bloch equations. The reader is referred to the quantum-optical treatment presented in Section 3.4 to deal with spontaneous emission as it cannot be understood semiclassically.

The two-level system is described by the Hamiltonian of the undisturbed system, H_0, and the Hamiltonian of an optical field coupling to the electronic transition dipole moment, $\hat{H}_L$:

$$\hat{H} = \hat{H}_0 + \hat{H}_L \tag{3.12}$$

with

$$\begin{aligned} \hat{H}_0 &= \epsilon_1 |1\rangle\langle 1| + \epsilon_2 |2\rangle\langle 2|, \\ \hat{H}_L &= -\mathbf{E}(t) \cdot \left\{ \mathbf{d}_{12} |1\rangle\langle 2| + \mathbf{d}_{21} |2\rangle\langle 1| \right\}, \end{aligned} \tag{3.13}$$

using the Schrödinger wave functions of state 1 and state 2, $|1\rangle$ and $|2\rangle$, respectively. The light field couples to the transition dipole moment of the system, see also Ref. [4], using the transition dipole matrix elements $\mathbf{d}_{12} = -e\langle 1|\hat{\mathbf{r}}|2\rangle$ and $\mathbf{d}_{21} = \mathbf{d}_{12}^* = -e\langle 2|\hat{\mathbf{r}}|1\rangle$. The Schrödinger equation for the system wave function $|\psi\rangle$ reads

$$i\hbar \frac{\mathrm{d}}{\mathrm{d}t} |\psi\rangle = \left[\hat{H}_0 + \hat{H}_L\right] |\psi\rangle. \tag{3.14}$$

The wave function $|\psi\rangle$ may be expanded in the eigenfunctions of the system,

$$|\psi\rangle = a_1(t) e^{-i\omega_1 t} |1\rangle + a_2(t) e^{-i\omega_2 t} |2\rangle, \tag{3.15}$$

using $\omega_1 = \epsilon_1/\hbar$ and $\omega_2 = \epsilon_2/\hbar$. Inserting this expansion into Equation 3.14 and multiplying with $\langle\psi|$ from the left-hand side yields equations for the coefficients $a_1(t)$ and $a_2(t)$,

$$\begin{aligned}\dot{a}_1(t) &= a_2(t)e^{-i(\omega_2-\omega_1)t}\langle 1|\hat{H}_\mathrm{L}|2\rangle,\\ \dot{a}_2(t) &= a_1(t)e^{-i(\omega_1-\omega_2)t}\langle 2|\hat{H}_\mathrm{L}|1\rangle.\end{aligned} \tag{3.16}$$

Applying a monochromatic incident field, $\mathbf{E}(t) = \frac{1}{2}\mathbf{E}_0(e^{-i\omega t} + e^{i\omega t})$, we derive

$$\begin{aligned}\dot{a}_1(t) &= \frac{a_2(t)}{2}\, e^{-i(\omega_2-\omega_1)t}\mathbf{E}_0\cdot\mathbf{d}_{21}(e^{-i\omega t} + e^{i\omega t}),\\ \dot{a}_2(t) &= \frac{a_1(t)}{2}\, e^{-i(\omega_1-\omega_2)t}\mathbf{E}_0\cdot\mathbf{d}_{12}(e^{-i\omega t} + e^{i\omega t}).\end{aligned} \tag{3.17}$$

Considering an optical field near the resonance frequency of the system ω_0, one of the addends in either equation is almost time independent and the other is oscillating quickly. In the rotating wave approximation (RWA), the latter term is ignored due to averaging out and we are left with

$$\begin{aligned}\dot{a}_1(t) &= \frac{a_2(t)}{2}\, e^{-i(\omega_0-\omega)t}\mathbf{E}_0\cdot\mathbf{d}_{12},\\ \dot{a}_2(t) &= \frac{a_1(t)}{2}\, e^{i(\omega_0-\omega)t}\mathbf{E}_0\cdot\mathbf{d}_{21}.\end{aligned} \tag{3.18}$$

For resonance conditions $\omega = \omega_0$, this system of coupled equations may easily be solved by time-differentiating the first equation and inserting the second, yielding

$$\frac{\mathrm{d}^2}{\mathrm{d}t^2}\, a_1(t) = -\frac{\left|\mathbf{E}_0\cdot\mathbf{d}_{12}\right|^2}{4} a_1(t). \tag{3.19}$$

Defining the Rabi frequency[†]

$$\Omega = \frac{\left|\mathbf{E}_0\cdot\mathbf{d}_{12}\right|}{\hbar}, \tag{3.20}$$

yields $a_1(t) = a_1(0)e^{\pm i\Omega t}$ as a solution to Equation 3.19, an equivalent expression for $a_2(t)$, and after resubstitution into Equation 3.15,

$$|\psi\rangle = a_1(0)e^{\pm i\Omega t}e^{-i\omega_1 t}|1\rangle + a_2(0)e^{\pm i\Omega t}e^{-i\omega_2 t}|2\rangle. \tag{3.21}$$

Starting with $a_1 = 0, a_2 = 1$, i.e., an electron in the excited state, we observe that the electron oscillates between ground and excited states with a cosine dependence and frequency Ω, describing the interplay between absorption and stimulated emission. These so-called *Rabi flops* are typical for any two-level system driven by an oscillatory field, including atoms in a light field as discussed here, but also particles in an oscillating magnetic field as investigated in nuclear magnetic resonance.

Looking at the optical processes possible in a two-level system with or without the incidence of light, we note the following: In the absence of the external perturbation represented by the laser pulse, the system is described by the Hamiltonian $\hat{H}_0$. If, at an initial time $t = 0$, it is in an eigenstate, it will remain in this state for any length of time. This applies to the ground state $|1\rangle$ as well as to the excited state $|2\rangle$.

[†] Named after American physicist Isidor Isaac Rabi (1898–1988).

It is, however, obviously not a realistic description, the reason for this being the absence of spontaneous emission in the semiclassical picture we used here. We see later that spontaneous emission enters the model with a quantization of light.

Now let us briefly consider the example of a laser system. Laser operation is basically as follows: An initial photon, usually produced by spontaneous emission, is confined to an active medium using a resonator and amplified by stimulated emission. Obviously, this will only work if stimulated emission exceeds absorption. Going back to Equation 3.10, we know that the Einstein coefficients for absorption and stimulated emission are equal and thus the occupancies of the ground and excited states govern the relative strength. Therefore, inversion has to be achieved for laser operation, i.e., the number of carriers in the excited state has to exceed the number of carriers in the ground state. Under certain conditions, quantum theory also allows lasing without inversion; since this requires intensive tailoring of the system, it will not be discussed here, but the reader is referred to the original literature, see, e.g., Refs. [5,6].

Unfortunately, inversion can, in general, not be achieved in a two-level system as there is no efficient pumping mechanism. Thus, a laser requires at least a three-level system for operation. The relevant equations for the three-level system may be derived in analogy to the case of the two-level system discussed here.

3.2.3 The Two-Level System in the Heisenberg Picture

We now introduce yet another description of the two-level system, changing from the Schrödinger picture to the Heisenberg picture. The passage from the Schrödinger picture to the Heisenberg picture is made by transferring the time dependence from the wave functions to the operator; for details, see any see any textbook on quantum mechanics. The formalism in this subsection is similar to the one in Section 3.3, which treats the many-body case. In this subsection, all calculations are presented in detail so the reader can reproduce them, while in Section 3.3, several steps are omitted for the sake of clarity and brevity.

The time evolution of the system in the Heisenberg picture is not governed by the Schrödinger equation any more, but by the Heisenberg equation of motion

$$\dot{\hat{\mathcal{O}}} = \frac{i}{\hbar}\left[\hat{H}, \hat{\mathcal{O}}\right], \tag{3.22}$$

where [.] denotes the commutator,

$$\left[\hat{H}, \hat{\mathcal{O}}\right] = \hat{H}\hat{\mathcal{O}} - \hat{\mathcal{O}}\hat{H}, \tag{3.23}$$

and $\hat{\mathcal{O}}$ is any operator.

The Heisenberg equation allows us to calculate the equation of motion for arbitrary operators. Here, we obviously only consider processes that conserve the number of carriers in the system. We revert to the formalism of second quantization mentioned in the introduction and introduce operators describing the electron. In the following, $\hat{c}_1$ ($\hat{c}_1^\dagger$) and $\hat{c}_2$ ($\hat{c}_2^\dagger$) describe annihilation (creation) operators for electrons in levels 1 and 2, respectively. The relevant particle-conserving two-operator quantities are thus $\hat{c}_1^\dagger\hat{c}_2$, $\hat{c}_2^\dagger\hat{c}_1$, $\hat{c}_1^\dagger\hat{c}_1$, and $\hat{c}_2^\dagger\hat{c}_2$. The first two quantities are the microscopic polarizations; it will be illustrated in Section 3.3 that the polarization is the relevant quantity when considering light–matter interaction. The latter two quantities $\hat{c}_1^\dagger\hat{c}_1$ and $\hat{c}_2^\dagger\hat{c}_2$ describe the carrier densities in levels 1 and 2, respectively. We observe that the equations of motion for these four quantities are coupled to each other, but form a closed system of equations.

The Hamiltonian $\hat{H} = \hat{H}_0 + \hat{H}_\mathrm{L}$ of the two-level system may be written as

$$\hat{H}_0 = \epsilon_1\hat{c}_1^\dagger\hat{c}_1 + \epsilon_2\hat{c}_2^\dagger\hat{c}_2,$$

$$\hat{H}_\mathrm{L} = -\mathbf{E}(t)\cdot(\mathbf{d}_{12}\hat{c}_1^\dagger\hat{c}_2 + \mathbf{d}_{21}\hat{c}_2^\dagger\hat{c}_1).$$

Inserting this Hamiltonian into the Heisenberg equation for the polarization $\hat{p} = \hat{c}_1^\dagger \hat{c}_2$, we derive the equation of motion for this quantity:

$$\begin{aligned}\dot{\hat{p}} &= \frac{i}{\hbar}\left[\hat{H}, \hat{p}\right] = \frac{i}{\hbar}\left(\hat{H}\hat{p} - \hat{p}\hat{H}\right) \\ &= \frac{i}{\hbar}\left\{\epsilon_1 \hat{c}_1^\dagger \hat{c}_1 + \epsilon_2 \hat{c}_2^\dagger \hat{c}_2 - \mathbf{E}(t)\cdot(\mathbf{d}_{12}\hat{c}_1^\dagger \hat{c}_2 + \mathbf{d}_{21}\hat{c}_2^\dagger \hat{c}_1)\right\} \hat{c}_1^\dagger \hat{c}_2 \\ &\quad - \hat{c}_1^\dagger \hat{c}_2 \left\{\epsilon_1 \hat{c}_1^\dagger \hat{c}_1 + \epsilon_2 \hat{c}_2^\dagger \hat{c}_2 - \mathbf{E}(t)\cdot(\mathbf{d}_{12}\hat{c}_1^\dagger \hat{c}_2 + \mathbf{d}_{21}\hat{c}_2^\dagger \hat{c}_1)\right\}. \end{aligned} \tag{3.24}$$

The goal now is to relate the time derivative of the polarization to known or accessible quantities. This may also be the polarization itself, enabling an analytical or a numerical solution of the resulting differential equation. To achieve this, we need to interchange the operators, e.g., bring them into normal ordering in every term.

First, we remind ourselves of the Fermionic anticommutators to be used here

$$\left\{\hat{c}_i^\dagger, \hat{c}_j\right\}_+ = \hat{c}_i^\dagger \hat{c}_j + \hat{c}_j \hat{c}_i^\dagger = \delta_{ij}, \tag{3.25}$$

$$\left\{\hat{c}_i^\dagger, \hat{c}_j^\dagger\right\}_+ = 0\,, \left\{\hat{c}_i, \hat{c}_j\right\}_+ = 0, \tag{3.26}$$

the rules for interchanging two operators thus being

$$\begin{aligned} &\hat{c}_i \hat{c}_j = -\hat{c}_j \hat{c}_i\,, \\ &\hat{c}_i^\dagger \hat{c}_j^\dagger = -\hat{c}_j^\dagger \hat{c}_i^\dagger\,, \\ &i \neq j \;\Rightarrow\; \hat{c}_i^\dagger \hat{c}_j = -\hat{c}_j \hat{c}_i^\dagger\,, \\ &i = j \;\Rightarrow\; \hat{c}_i^\dagger \hat{c}_i = \hat{1} - \hat{c}_i \hat{c}_i^\dagger \end{aligned}$$

using the identity operator $\hat{1}$. The first two relations also show that the square of any Fermionic operator equals zero,

$$\hat{c}_i^\dagger \hat{c}_i^\dagger = \hat{c}_i \hat{c}_i = 0, \tag{3.27}$$

resulting from the Pauli principle[†] stating that no two fermions may occupy the same state.

From Equation 3.24, we calculate

$$\begin{aligned} -i\hbar\dot{\hat{p}} &= \left(\epsilon_1 \hat{c}_1^\dagger \hat{c}_1 \hat{c}_1^\dagger \hat{c}_2 + \epsilon_2 \hat{c}_2^\dagger \hat{c}_2 \hat{c}_1^\dagger \hat{c}_2 - \mathbf{E}(t)\cdot(\mathbf{d}_{12}\hat{c}_1^\dagger \hat{c}_2 \hat{c}_1^\dagger \hat{c}_2 + \mathbf{d}_{21}\hat{c}_2^\dagger \hat{c}_1 \hat{c}_1^\dagger \hat{c}_2)\right) \\ &\quad - \left(\epsilon_1 \hat{c}_1^\dagger \hat{c}_2 \hat{c}_1^\dagger \hat{c}_1 + \epsilon_2 \hat{c}_1^\dagger \hat{c}_2 \hat{c}_2^\dagger \hat{c}_2 - \mathbf{E}(t)\cdot(\mathbf{d}_{12}\hat{c}_1^\dagger \hat{c}_2 \hat{c}_1^\dagger \hat{c}_2 + \mathbf{d}_{21}\hat{c}_1^\dagger \hat{c}_2 \hat{c}_2^\dagger \hat{c}_1)\right) \\ &= \left(\epsilon_1 \hat{c}_1^\dagger \hat{c}_1 \hat{c}_1^\dagger \hat{c}_2 - \epsilon_1 \hat{c}_1^\dagger \hat{c}_2 \hat{c}_1^\dagger \hat{c}_1 + \epsilon_2 \hat{c}_2^\dagger \hat{c}_2 \hat{c}_1^\dagger \hat{c}_2 - \epsilon_2 \hat{c}_1^\dagger \hat{c}_2 \hat{c}_2^\dagger \hat{c}_2\right) \\ &\quad - \mathbf{E}(t)\cdot\left(\mathbf{d}_{21}\hat{c}_2^\dagger \hat{c}_1 \hat{c}_1^\dagger \hat{c}_2 - \mathbf{d}_{21}\hat{c}_1^\dagger \hat{c}_2 \hat{c}_2^\dagger \hat{c}_1\right), \end{aligned}$$

[†] Named after Austrian-born Swiss and American physicist Wolfgang Pauli (1900–1958).

and, commuting the terms into normal order by using the Fermionic anticommutators,

$$-i\hbar\dot{\hat{p}} = \left(\epsilon_1\hat{c}_1^\dagger(\hat{1}-\hat{c}_1^\dagger\hat{c}_1)\hat{c}_2 + \epsilon_1\hat{c}_1^\dagger\hat{c}_1^\dagger\hat{c}_2\hat{c}_1 - \epsilon_2\hat{c}_2^\dagger\hat{c}_1^\dagger\hat{c}_2\hat{c}_2 - \epsilon_2\hat{c}_1^\dagger(\hat{1}-\hat{c}_2^\dagger\hat{c}_2)\hat{c}_2\right)$$
$$-\mathbf{E}(t)\cdot\mathbf{d}_{21}\left(\hat{c}_2^\dagger(\hat{1}-\hat{c}_1^\dagger\hat{c}_1)\hat{c}_2 - \hat{c}_1^\dagger(\hat{1}-\hat{c}_2^\dagger\hat{c}_2)\hat{c}_1\right). \tag{3.28}$$

The four-operator terms either cancel or disappear due to Equation 3.27 and we are left with

$$-i\hbar\dot{\hat{p}} = \left(\epsilon_1\hat{c}_1^\dagger\hat{c}_2 - \epsilon_2\hat{c}_1^\dagger\hat{c}_2\right) - \mathbf{E}(t)\cdot\mathbf{d}_{21}\left(\hat{c}_2^\dagger\hat{c}_2 - \hat{c}_1^\dagger\hat{c}_1\right)$$
$$= \left(\epsilon_1-\epsilon_2\right)\hat{p} + \mathbf{E}(t)\cdot\mathbf{d}_{21}\left(\hat{n}_1-\hat{n}_2\right). \tag{3.29}$$

Obviously, this equation couples to the equations for the occupation of the two levels, $\hat{n}_1 = \hat{c}_1^\dagger\hat{c}_1$, $\hat{n}_2 = \hat{c}_2^\dagger\hat{c}_2$. Deriving the equations of motion for these quantities in the same way, defining the energy difference in the system as $\hbar\omega_0 = \epsilon_2 - \epsilon_1$ as before and taking the expectation values lead to the optical Bloch equations (also called Maxwell–Bloch equations)

$$\begin{aligned} -i\hbar\dot{p} + \hbar\omega_0 p &= \mathbf{E}(t)\cdot\mathbf{d}_{21}(n_1-n_2),\\ -i\hbar\dot{n}_1 &= \mathbf{E}(t)\cdot(\mathbf{d}_{12}p - \mathbf{d}_{21}p^*),\\ -i\hbar\dot{n}_2 &= \mathbf{E}(t)\cdot(\mathbf{d}_{21}p^* - \mathbf{d}_{12}p). \end{aligned}$$

These equations are completely analogous to the Bloch equations in spin-$\frac{1}{2}$-systems (where a two-level system in this chapter is not to be understood as a two-level system containing electrons *with* spin but rather as a model system whose Hilbert space is isomorphic to a spin-$\frac{1}{2}$-system).

Let us now briefly discuss the electron–hole picture at this level. Starting from the ground state where the electrons are in level 1, often only a small fraction of the electrons is lifted to the upper level. It is then frequently advantageous to count the empty spaces in the ground state rather than the electrons. These "holes" carry positive charge because the missing electron implies lack of compensation of nuclear charge. We define

$$\begin{aligned} n_2 &= n_e && \text{upper level}\\ n_1 &= 1-n_h && \text{lower level}\\ n_1+n_2 &= 1 && \Rightarrow n_e = n_h \equiv n \end{aligned}$$

and rewrite the optical Bloch equations

$$\begin{aligned} \dot{p} &= -i\omega_0 p + \tfrac{i}{\hbar}\mathbf{E}(t)\cdot\mathbf{d}_{21}(1-2n),\\ \dot{n} &= \tfrac{i}{\hbar}\mathbf{E}(t)\cdot(\mathbf{d}_{21}p - \mathbf{d}_{12}p^*). \end{aligned}$$

For low excitation powers, where the predominant part of the carriers stays in the lower level, n may be neglected (linear case, $n \approx 0$) and a single equation of motion for the polarization remains

$$\dot{p} = -i\omega_0 p + \frac{i}{\hbar}\mathbf{E}(t)\cdot\mathbf{d}_{21}. \tag{3.30}$$

Solving this for a specific light field, one discovers that even after the end of excitation, the polarization remains forever, the reason being that relaxation processes have been neglected thus far. This may be remedied by introducing a phenomenological damping into the equations of motion

$$\begin{aligned} \dot{p} &= -i\omega_0 p + \tfrac{i}{\hbar}\mathbf{E}(t)\cdot\mathbf{d}_{21}(1-2n) - \tfrac{p}{T_2},\\ \dot{n} &= \tfrac{i}{\hbar}\mathbf{E}(t)\cdot(\mathbf{d}_{21}p - \mathbf{d}_{12}p^*) - \tfrac{n}{T_1}, \end{aligned}$$

where T_1 and T_2 are relaxation times, which are usually derived by fits to experiment. The inclusion of relaxation times results in a broadening of the spectrum, which is called homogeneous because all emitters experience the same type of broadening mechanism; see Ref. [2]. The counterpart to this mechanism is inhomogeneous broadening, which is caused by disorder; see also Section 3.3; here, different emitters experience different environmental influences.

We now solve the polarization equation of motion in the relaxation time approach to illustrate that it leads to a Lorentzian lineshape of the polarization and absorption spectrum. Defining $\Gamma = 1/T_2$, we calculate

$$\frac{\mathrm{d}}{\mathrm{d}t}\left\{pe^{(i\omega_0+\Gamma)t}\right\} = \frac{i}{\hbar}\mathbf{E}(t)\cdot\mathbf{d}_{21}(1-2n(t))e^{(i\omega_0+\Gamma)t} \tag{3.31}$$

and formally integrate this equation, deriving

$$p(t) = \frac{i}{\hbar}\int_{-\infty}^{t}\mathrm{d}t' e^{(i\omega_0+\Gamma)(t'-t)}\mathbf{E}(t')\cdot\mathbf{d}_{21}(1-2n(t')). \tag{3.32}$$

We now insert a monochromatic incident field

$$\mathbf{E}(t) = \frac{1}{2}\mathbf{E}_0\left\{e^{-i\omega t}+e^{i\omega t}\right\} \tag{3.33}$$

and assume a quasistationary or stationary state of the system, i.e., the carrier density changes little on the timescale of T_2. We may then replace $n(t')$ by $n(t)$ and get

$$p(t) = \frac{i}{2\hbar}\mathbf{E}_0\cdot\mathbf{d}_{21}(1-2n(t))\int_{-\infty}^{t}\mathrm{d}t' e^{(i\omega_0+\Gamma)(t'-t)}\left\{e^{-i\omega t'}+e^{i\omega t'}\right\}. \tag{3.34}$$

This replacement actually means that the prediction of the system behavior is made based only on the present state and not on the history of the system. This is a so-called "memoryless" process obtained using the Markov approximation.

The integral in Equation 3.34 may now be solved, yielding

$$\begin{aligned}
p(t) &= \frac{i}{2\hbar}\mathbf{E}_0\cdot\mathbf{d}_{21}(1-2n(t))e^{-(i\omega_0+\Gamma)t}\int_{-\infty}^{t}\mathrm{d}t'\left\{e^{(i(\omega_0-\omega)+\Gamma)t'}+e^{(i(\omega_0+\omega)+\Gamma)t'}\right\}\\
&= \frac{i}{2\hbar}\mathbf{E}_0\cdot\mathbf{d}_{21}(1-2n(t))e^{-(i\omega_0+\Gamma)t}\left[\frac{e^{(i(\omega_0-\omega)+\Gamma)t'}}{i(\omega_0-\omega)+\Gamma}+\frac{e^{(i(\omega_0+\omega)+\Gamma)t'}}{i(\omega_0+\omega)+\Gamma}\right]_{-\infty}^{t}\\
&= \frac{i}{2\hbar}\mathbf{E}_0\cdot\mathbf{d}_{21}(1-2n(t))e^{-(i\omega_0+\Gamma)t}\left\{\frac{e^{(i(\omega_0-\omega)+\Gamma)t}}{i(\omega_0-\omega)+\Gamma}+\frac{e^{(i(\omega_0+\omega)+\Gamma)t}}{i(\omega_0+\omega)+\Gamma}\right\}.
\end{aligned} \tag{3.35}$$

Considering resonant or near-resonant excitation, the denominator $i(\omega_0+\omega)+\Gamma$ can be considered as large and the second addend may be neglected. This corresponds to the RWA, which was already used in getting from Equation 3.17 to 3.18 in Section 3.2.2. We are left with

$$p(t) = \frac{i}{2\hbar}\mathbf{E}_0 e^{-i\omega t}\cdot\mathbf{d}_{21}(1-2n(t))\frac{1}{i(\omega_0-\omega)+\Gamma}. \tag{3.36}$$

In the last fraction of Equation 3.36, $(i(\omega_0-\omega)+\Gamma)^{-1}$, the Lorentzian lineshape of the absorption spectrum becomes apparent, the absorption being approximately proportional to the imaginary part of the

expression (see Ref. [7,8], Equation 3.53 in this chapter) and

$$\frac{1}{i(\omega_0-\omega)+\Gamma}=\frac{\Gamma}{(\omega_0-\omega)^2+\Gamma^2}+i\frac{\omega_0-\omega}{(\omega_0-\omega)^2+\Gamma^2}. \tag{3.37}$$

In Section 3.3, we discuss the drawbacks of the relaxation time approach. Generally, it constitutes a simple and easily comprehensible procedure, where, however, the relaxation times must be inserted by hand and are not calculated by the theory.

3.3 The Solid-State System

We now move on to a much more complex system, the semiconductor. Not only do we encounter a system of many atoms forming an energy landscape known as band structure here (see also Chapter 1), but, in addition, we also need to take into account a large number of electrons. However, a semiconductor is what the diodes, amplifiers, laser diodes, optical modulators, and solar cells discussed in this book are made out of. In order to get a flavor of a many-body treatment of electron–photon interaction, the derivation of the semiconductor Bloch equations will be discussed briefly here. For an in-depth treatment, the reader is referred to Ref. [7], the references therein, and a wealth of original literature. Since a many-body problem can only be solved approximately, for every case the equations have to be examined separately and the proper approximations made. This is far beyond the scope of this chapter.

In optoelectronics, we customarily deal with direct-bandgap semiconductors. Here, we consider the simplest possible case, a direct-gap two-band semiconductor and derive the relevant equations of motion. It comprises a valence and a conduction band, where in the ground state, all the electrons are in the valence band and fill up its states completely. Similar to the two-level system, they may be raised to the conduction band by optical excitation. Figure 3.2 shows a simplified schematic of the direct-gap two-band semiconductor. Equations of motion for more complicated systems may be obtained by expanding the indices in the derivation below to all the existing bands; a derivation for a multiband system is thus straightforward but more cumbersome.

Looking at the semiconductor–light interaction, we need to keep in mind that the size of an atom is in the range of a single Ångström, while the wavelength of visible light is approximately 400–700 nm, i.e., 4000–7000 Ångström. The electric field is thus approximately constant over the extension of a single atom, and all quantities in Maxwell's equations† are averaged over a large number of atoms.

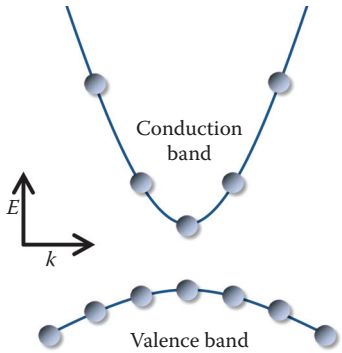

FIGURE 3.2 Schematic of a two-band direct-gap semiconductor.

† Named after Scottish physicist James Clerk Maxwell (1831–1879).

The Hamiltonian of the solid-state system is made up of three contributions,

$$\hat{H} = \hat{H}_{el} + \hat{H}_{\mathrm{L}} = (\hat{H}_0 + \hat{H}_C) + \hat{H}_{\mathrm{L}}, \tag{3.38}$$

where $\hat{H}_{el}$ is the Hamiltonian of the electronic system, consisting of the sum of the individual single particle contributions, $\hat{H}_0$, and the Coulomb interaction between the electrons, $\hat{H}_C$. As before, $\hat{H}_{\mathrm{L}}$ denotes the interaction with the light field.

The structure of an inorganic semiconductor is characterized by its crystallinity, i.e., periodicity. In other words, the environment of an electron is the same in position $\mathbf{r}$ and position $\mathbf{r}+\mathbf{R}_n$, where $\mathbf{R}_n$ is any lattice vector, i.e., a vector linking two identical sites in an infinite lattice. The periodicity is taken into account in the Bloch theorem† for the wave functions,

$$\psi_\lambda(\mathbf{k}, \mathbf{r}+\mathbf{R}_n) = e^{i\mathbf{k}\cdot\mathbf{R}_n}\psi_\lambda(\mathbf{k}, \mathbf{r}). \tag{3.39}$$

Consequently, the Hamiltonian is expanded in electronic Bloch wave functions,

$$\psi_\lambda(\mathbf{k}, \mathbf{r}) \approx \mathrm{e}^{i\mathbf{k}\cdot\mathbf{r}}\,\frac{u_\lambda(\mathbf{k}, \mathbf{r})}{L^{\frac{3}{2}}}. \tag{3.40}$$

L^3 is the volume of the crystal and λ denotes the band index, comprising the conduction band $\lambda = c$ and the valence band $\lambda = v$. Bloch functions take into account the lattice periodicity of the system by including a lattice periodic function $u_\lambda(\mathbf{k}, \mathbf{r})$,

$$u_\lambda(\mathbf{k}, \mathbf{r}+\mathbf{R}_n) = u_\lambda(\mathbf{k}, \mathbf{r}). \tag{3.41}$$

The introduction of the crystal volume L^3 necessitates further explanation, as Equation 3.39 is only valid in an infinite system. Customary crystals are so large that the assumption of infinity is quite fitting. Since for a proper normalization of the wave functions, one needs a finite crystal volume, we consider the (approximately infinite) crystal to be made up of mesoscopic cubes of size L^3 and demand periodic boundary conditions of the wave function, i.e., the wave function has to have the same value on either side of the cube.

For the single particle contribution, we derive

$$\begin{aligned}\hat{H}_0 &= \sum_{\mathbf{k},\lambda=v,c} \epsilon_\lambda(\mathbf{k})\,\hat{c}^\dagger_{\lambda,\mathbf{k}}\hat{c}_{\lambda,\mathbf{k}} \\ &= \sum_{\mathbf{k}} \epsilon_v(\mathbf{k})\,\hat{c}^\dagger_{v,\mathbf{k}}\hat{c}_{v,\mathbf{k}} + \sum_{\mathbf{k}} \epsilon_c(\mathbf{k})\,\hat{c}^\dagger_{c,\mathbf{k}}\hat{c}_{c,\mathbf{k}}.\end{aligned} \tag{3.42}$$

$\hat{c}_{\lambda,\mathbf{k}}$ ($\hat{c}^\dagger_{\lambda,\mathbf{k}}$) is the annihilation (creation) operator of an electron in state $\lambda, \mathbf{k}$.

Since the energies $\epsilon_\lambda(\mathbf{k})$ are rather difficult to assess, parabolic bands are often assumed, corresponding to the effective mass approximation. At the extrema of the band structure, the linear term in the Taylor expansion becomes zero, such that a parabolic approximation may be made. Formally, a constant called the "effective mass," $m_{\lambda,\mathrm{eff}} = \frac{\hbar^2}{\left.\frac{\partial^2\epsilon_\lambda(\mathbf{k})}{\partial k^2}\right|_{k=0}}$, may then be introduced,

$$\begin{aligned}\epsilon_\lambda(\mathbf{k}) &= \epsilon_\lambda(\mathbf{k}=0) + \frac{1}{2}\frac{\partial^2\epsilon_\lambda(\mathbf{k})}{\partial k^2} + O(k^3) \\ &\approx \epsilon_\lambda(\mathbf{k}=0) + \frac{\hbar^2 k^2}{2m_{\lambda,\mathrm{eff}}}.\end{aligned} \tag{3.43}$$

† Named after Swiss physicist Felix Bloch (1905–1983).

Here, $O(k^3)$ denotes higher-order terms. For the Bloch functions, this implies that the lattice-periodic part becomes momentum independent, i.e., $u_\lambda(\mathbf{k}, \mathbf{r}) \approx u_\lambda(\mathbf{k} = 0, \mathbf{r})$. This approximation is always valid in a certain range around an extremum of the band structure but is used extensively in calculations even far away from these points. In the effective-mass approximation, the electrons behave like free particles with the effective mass $m_{\lambda,\text{eff}}$ rather than the free-particle mass. $m_{\lambda,\text{eff}}$ may be positive or negative, examples being the conduction and valence band in the case of the two-band semiconductor we are looking at. When the sign is negative, this is often included into the energy by transferring to the electron–hole picture. Furthermore, the effective mass, in general, is not independent of direction and must be written as a tensor,

$$\left(\frac{1}{m_{\lambda,\text{eff}}}\right)_{\alpha\beta} = \frac{1}{\hbar^2}\left.\frac{\partial^2 \epsilon_\lambda(\mathbf{k})}{\partial k_\alpha k_\beta}\right|_{k=0}. \tag{3.44}$$

The direction dependence of the effective mass is discussed, e.g., in Refs. [9–11].

Returning to light–matter coupling in semiconductors, we have seen that light couples to electrical dipoles,

$$\hat{H}_\text{L} = -\mathbf{E}(t) \cdot (e\hat{\mathbf{r}}) = -\mathbf{E}(t) \cdot \hat{\mathbf{d}}\,. \tag{3.45}$$

Expanding the interaction Hamiltonian in these wave functions yields

$$\begin{aligned}
\hat{H}_\text{L} &= -e\,\mathbf{E}(t) \cdot \sum_{\mathbf{k},\lambda,\lambda'} \left\langle \lambda', \mathbf{k}\right| \mathbf{r} \left|\lambda, \mathbf{k}\right\rangle \hat{c}^\dagger_{\lambda',\mathbf{k}} \hat{c}_{\lambda,\mathbf{k}} \\
&= -\mathbf{E}(t) \cdot \left[\sum_{\mathbf{k},\lambda,\lambda',\lambda\neq\lambda'} \mathbf{d}_{\lambda',\lambda}(\mathbf{k})\, \hat{c}^\dagger_{\lambda',\mathbf{k}} \hat{c}_{\lambda,\mathbf{k}}\right] \\
&= -\mathbf{E}(t) \cdot \sum_{\mathbf{k}} \left[\mathbf{d}_{cv}(\mathbf{k})\, \hat{c}^\dagger_{c,\mathbf{k}} \hat{c}_{v,\mathbf{k}} + \mathbf{d}_{vc}(\mathbf{k})\, \hat{c}^\dagger_{v,\mathbf{k}} \hat{c}_{c,\mathbf{k}}\right] \\
&= -\mathbf{E}(t) \cdot \hat{\mathbf{P}}\,,
\end{aligned} \tag{3.46}$$

where $\hat{\mathbf{P}}$ is the optical interband polarization. $\mathbf{d}_{\lambda',\lambda}(\mathbf{k})$ are the band and momentum-dependent optical transition dipole matrix elements with in-plane momentum $\mathbf{k}$ and subband labels λ, λ', corresponding to the transition dipole matrix elements $\mathbf{d}_{12}, \mathbf{d}_{21}$ in the two-level system.

To obtain Equation 3.46, the following approximations are made: (1) the photon momentum is neglected and (2) intraband transitions are not considered. Rather than retracing the entire derivation,[†] let us discuss these approximations:

1. Neglect of the photon momentum: In this book, we concentrate on light in and around the visible range, i.e., with wavelengths roughly between 400 and 700 nm. For a central wavelength of 550 nm, the wave number is $k = 2\pi/\lambda = 11 \times 10^6\ \text{m}^{-1}$, which is very small compared to typical wave vectors in a semiconductor band structure. Photonic transitions are consequently vertical in a band diagram.
2. Neglect of intraband transitions: Here, only interband transitions will be considered, assuming an excitation at an energy near the band gap. Suppression of intraband transitions in a regular structure becomes obvious from the vanishing photon momentum as discussed earlier.

Looking at the system Hamiltonian, Equation 3.38, we still need to calculate the term $\hat{H}_C$ describing Coulomb interaction between the carriers. $\hat{H}_C$ is specified using the so-called jellium model, which

[†] See Ref. [7] for details.

substitutes the ionic background of the lattice with a smooth background. The derivation is not included here, but may be found in Ref. [7]. The final expression of the Hamiltonian is

$$\begin{aligned}\hat{H}_C &= \sum_{\mathbf{k},\mathbf{k}',\mathbf{q}\neq 0,\lambda,\lambda'=v,c} V_q\, \hat{c}^\dagger_{\lambda,\mathbf{k}+\mathbf{q}} \hat{c}^\dagger_{\lambda',\mathbf{k}'-\mathbf{q}} \hat{c}_{\lambda',\mathbf{k}'} \hat{c}_{\lambda,\mathbf{k}} \\ &= \sum_{\mathbf{k},\mathbf{k}',\mathbf{q}\neq 0} V_q \left[\hat{c}^\dagger_{v,\mathbf{k}+\mathbf{q}} \hat{c}^\dagger_{v,\mathbf{k}'-\mathbf{q}} \hat{c}_{v,\mathbf{k}'} \hat{c}_{v,\mathbf{k}} + \hat{c}^\dagger_{c,\mathbf{k}+\mathbf{q}} \hat{c}^\dagger_{c,\mathbf{k}'-\mathbf{q}} \hat{c}_{c,\mathbf{k}'} \hat{c}_{c,\mathbf{k}} + 2\hat{c}^\dagger_{c,\mathbf{k}+\mathbf{q}} \hat{c}^\dagger_{v,\mathbf{k}'-\mathbf{q}} \hat{c}_{v,\mathbf{k}'} \hat{c}_{c,\mathbf{k}} \right], \end{aligned} \tag{3.47}$$

where the second line spells out the interaction for our two-band model. $\hat{H}_C$ thus describes the repulsion between electrons in the valence band, electrons in the conduction band and between valence and conduction band. V_q is the Fourier transform of the Coulomb potential,

$$V(\mathbf{r}) = \frac{e^2}{4\pi\mathcal{E}_0\mathcal{E}_r r}, \tag{3.48}$$

$$V_q = \int \frac{\mathrm{d}^3 r}{L^3} V(\mathbf{r}) \mathrm{e}^{i\mathbf{q}\cdot\mathbf{r}} = \frac{e^2}{\mathcal{E}_0\mathcal{E}_r L^3 q^2}, \tag{3.49}$$

where for the calculation a convergence generating factor needs to be used. $\mathcal{E}_0$ and $\mathcal{E}_r$ are the vacuum and relative material permittivity, respectively. The sum in Equation 3.47 omits the case $\mathbf{q} = 0$ where obviously the Coulomb matrix element has a singularity; this term is canceled by the ionic background charge in the jellium model.

The complete Hamiltonian is thus

$$\begin{aligned}\hat{H} &= \hat{H}_0 + \hat{H}_C + \hat{H}_\mathrm{L} \\ &= \sum_{\mathbf{k},\lambda=v,c} \epsilon_\lambda(\mathbf{k})\, \hat{c}^\dagger_{\lambda,\mathbf{k}} \hat{c}_{\lambda,\mathbf{k}} + \sum_{\mathbf{k},\mathbf{k}',\mathbf{q}\neq 0,\lambda,\lambda'=v,c} V_q\, \hat{c}^\dagger_{\lambda,\mathbf{k}+\mathbf{q}} \hat{c}^\dagger_{\lambda',\mathbf{k}'-\mathbf{q}} \hat{c}_{\lambda',\mathbf{k}'} \hat{c}_{\lambda,\mathbf{k}} \\ &\quad - \mathbf{E}(t) \cdot \left[\sum_{\mathbf{k},\lambda,\lambda',\lambda\neq\lambda'} \mathbf{d}_{\lambda',\lambda}(\mathbf{k},\mathbf{k})\, \hat{c}^\dagger_{\lambda',\mathbf{k}} \hat{c}_{\lambda,\mathbf{k}} \right]. \end{aligned} \tag{3.50}$$

This Hamiltonian is now going to be used for the calculation of the optical polarization $\hat{\mathbf{P}}$,

$$\begin{aligned}\hat{\mathbf{P}} &= \sum_{\mathbf{k}} \left(\mathbf{d}_{vc}\, \hat{c}^\dagger_{v,\mathbf{k}} \hat{c}_{c,\mathbf{k}} + \mathbf{d}_{cv}\, \hat{c}^\dagger_{c,\mathbf{k}} \hat{c}_{v,\mathbf{k}} \right) \\ &= \sum_{\mathbf{k}} \left(\mathbf{d}_{vc}\, \hat{c}^\dagger_{v,\mathbf{k}} \hat{c}_{c,\mathbf{k}} + \text{h.c.} \right) = \sum_{\mathbf{k}} \left(\mathbf{d}_{vc}\, \hat{p}_{vc,\mathbf{k}} + \text{h.c.} \right), \end{aligned} \tag{3.51}$$

where $p_{vc,\mathbf{k}} = \langle \hat{p}_{vc,\mathbf{k}} \rangle$ are the microscopic interband coherences or polarizations and h.c. denotes the Hermitian conjugate. The optical polarization is a quantity that describes the reaction of matter to a light field, coupling light (electric field $\mathbf{E}(\mathbf{r}, t)$) to matter in the wave equation

$$\Delta\mathbf{E}(\mathbf{r}, t) - \left(\frac{n}{c}\right)^2 \frac{\partial^2}{\partial t^2} \mathbf{E}(\mathbf{r}, t) = \mu_0 \frac{\partial^2}{\partial t^2} \mathbf{P}(\mathbf{r}, t) \tag{3.52}$$

with the index of refraction n and the vacuum permeability μ_0. The optical polarization is a fundamental parameter from which numerous optical variables can be calculated, e.g., the absorption α or laser gain g being given as

$$\alpha(\omega) = -g(\omega) = \frac{\omega}{nc} \mathrm{Im} \left\{ \frac{P(\omega)}{L^3 E(\omega)} \right\}, \tag{3.53}$$

see Ref. [8]. In Equation 3.53, the index of refraction n was assumed to be constant in the region of interest. Calculation of the optical polarization thus gives us deep insight into the optical properties of matter and allows us to simulate optical devices such as the ones discussed in this book.

Returning to the actual calculation of the optical polarization, the next step is the insertion of the many-body Hamiltonian into the Heisenberg equation of motion for the microscopic polarizations

$$\frac{\mathrm{d}}{\mathrm{d}t}\hat{c}^{\dagger}_{v,\mathbf{k}}\hat{c}_{c,\mathbf{k}} = \frac{i}{\hbar}\left[\hat{H}, \hat{c}^{\dagger}_{v,\mathbf{k}}\hat{c}_{c,\mathbf{k}}\right]. \tag{3.54}$$

Calculating the appropriate commutators and taking the expectation values on both sides renders

$$\begin{aligned}\left[i\hbar\frac{\mathrm{d}}{\mathrm{d}t} - (\epsilon_c(\mathbf{k}) - \epsilon_v(\mathbf{k}))\right] p_{vc,\mathbf{k}} &= (n_{c,\mathbf{k}} - n_{v,\mathbf{k}})\mathbf{d}_{cv}\cdot\mathbf{E}(t) \\ &+ \sum_{\mathbf{k}',\mathbf{q}\neq 0} V_q \Big[\langle \hat{c}^{\dagger}_{c,\mathbf{k}'+\mathbf{q}}\hat{c}^{\dagger}_{v,\mathbf{k}-\mathbf{q}}\hat{c}_{c,\mathbf{k}'}\hat{c}_{c,\mathbf{k}}\rangle + \langle \hat{c}^{\dagger}_{v,\mathbf{k}'+\mathbf{q}}\hat{c}^{\dagger}_{v,\mathbf{k}-\mathbf{q}}\hat{c}_{v,\mathbf{k}'}\hat{c}_{c,\mathbf{k}}\rangle \\ &\quad + \langle \hat{c}^{\dagger}_{v,\mathbf{k}}\hat{c}^{\dagger}_{c,\mathbf{k}'-\mathbf{q}}\hat{c}_{c,\mathbf{k}'}\hat{c}_{c,\mathbf{k}-\mathbf{q}}\rangle + \langle \hat{c}^{\dagger}_{v,\mathbf{k}}\hat{c}^{\dagger}_{v,\mathbf{k}'-\mathbf{q}}\hat{c}_{v,\mathbf{k}'}\hat{c}_{c,\mathbf{k}-\mathbf{q}}\rangle\Big],\end{aligned} \tag{3.55}$$

where $n_{c,\mathbf{k}} = \langle \hat{c}^{\dagger}_{c,\mathbf{k}}\hat{c}_{c,\mathbf{k}}\rangle$ and $n_{v,\mathbf{k}} = \langle \hat{c}^{\dagger}_{v,\mathbf{k}}\hat{c}_{v,\mathbf{k}}\rangle$ are the carrier densities in the conduction and valence band, respectively. The transition dipole matrix element was assumed to be real, $\mathbf{d}_{cv} = \mathbf{d}_{vc}$.

Obviously, the polarization as a two-operator quantity on the left-hand side of Equation 3.55 couples to four-operator quantities on the right side via the Coulomb interaction. Computing the equation of motion for these four-operator terms will in turn lead to a coupling to six-operator quantities, which will then couple to eight-operator quantities and so on, with ever-rising computational cost. This so-called *infinite hierarchy problem*, which is an expression of the many-body character of the electron system, necessitates a truncation at some level. A relatively simple approximation at two-operator level is the dynamic Hartree–Fock approximation.[†] Roughly speaking, it assumes that any particle experiences the impact of all other particles as a mean field created by them. Technically, in Hartree–Fock approximation, we split four-operator quantities into all possible combinations of two-operator quantities. For example, the first Coulomb term of Equation 3.55 yields

$$\begin{aligned}\langle \hat{c}^{\dagger}_{c,\mathbf{k}'+\mathbf{q}}\hat{c}^{\dagger}_{v,\mathbf{k}-\mathbf{q}}\hat{c}_{c,\mathbf{k}'}\hat{c}_{c,\mathbf{k}}\rangle &\approx \langle \hat{c}^{\dagger}_{c,\mathbf{k}'+\mathbf{q}}\hat{c}_{c,\mathbf{k}}\rangle\langle \hat{c}^{\dagger}_{v,\mathbf{k}-\mathbf{q}}\hat{c}_{c,\mathbf{k}'}\rangle - \langle \hat{c}^{\dagger}_{c,\mathbf{k}'+\mathbf{q}}\hat{c}_{c,\mathbf{k}'}\rangle\langle \hat{c}^{\dagger}_{v,\mathbf{k}-\mathbf{q}}\hat{c}_{c,\mathbf{k}}\rangle \\ &\approx \delta_{\mathbf{k},\mathbf{k}'+\mathbf{q}}\langle \hat{c}^{\dagger}_{c,\mathbf{k}}\hat{c}_{c,\mathbf{k}}\rangle\langle \hat{c}^{\dagger}_{v,\mathbf{k}-\mathbf{q}}\hat{c}_{c,\mathbf{k}-\mathbf{q}}\rangle - \delta_{\mathbf{k}',\mathbf{k}'-\mathbf{q}}\langle \hat{c}^{\dagger}_{c,\mathbf{k}'}\hat{c}_{c,\mathbf{k}'}\rangle\langle \hat{c}^{\dagger}_{v,\mathbf{k}}\hat{c}_{c,\mathbf{k}}\rangle \\ &= \delta_{\mathbf{k},\mathbf{k}'+\mathbf{q}} n_{c,\mathbf{k}} p_{vc,\mathbf{k}-\mathbf{q}},\end{aligned}$$

using $\mathbf{q} \neq 0$. In the second and third lines, we have taken into account that only terms that are diagonal in momentum are excited in a spatially homogeneous system. Approximating the other terms likewise, the resulting equation of motion for $p_{vc,\mathbf{k}}$ is

$$\left[i\hbar\frac{\mathrm{d}}{\mathrm{d}t} - (e_c(\mathbf{k}) - e_v(\mathbf{k}))\right] p_{vc,\mathbf{k}} = [n_{c,\mathbf{k}} - n_{v,\mathbf{k}}]\left(\mathbf{d}_{cv}\cdot\mathbf{E}(t) + \sum_{\mathbf{q}\neq\mathbf{k}} V_{|\mathbf{k}-\mathbf{q}|} p_{vc,\mathbf{q}}\right), \tag{3.56}$$

[†] Named after English mathematician and physicist Douglas Rayner Hartree (1897–1958) and Soviet physicist Vladimir Aleksandrovich Fock (1898–1974).

with renormalized energies

$$e_\lambda(\mathbf{k}) = \epsilon_\lambda(\mathbf{k}) - \sum_{\mathbf{q}\neq\mathbf{k}} V_{|\mathbf{k}-\mathbf{q}|} n_{\lambda,\mathbf{q}} \equiv \epsilon_\lambda(\mathbf{k}) + \Sigma_{exc,\lambda}(\mathbf{k}), \tag{3.57}$$

where $\Sigma_{exc}(\mathbf{k})$ is the exchange self-energy.

Equation 3.56 is not yet closed, but couples to the carrier densities $n_{c,\mathbf{k}}$, $n_{v,\mathbf{k}}$. To close the system of equations, the equations of motion for these quantities are derived in analogy to the prior derivation of Equation 3.56, and the following equations are obtained:

$$\frac{\mathrm{d}}{\mathrm{d}t} n_{c,\mathbf{k}} = -\frac{\mathrm{d}}{\mathrm{d}t} n_{v,\mathbf{k}} = -\frac{2}{\hbar}\,\mathrm{Im}\left[(\mathbf{d}_{cv}\cdot\mathbf{E}(t) + \sum_{\mathbf{q}\neq\mathbf{k}} V_{|\mathbf{k}-\mathbf{q}|} p_{vc,\mathbf{q}}) p^*_{vc,\mathbf{k}}\right]. \tag{3.58}$$

We now have a closed system of equations for $p_{vc,\mathbf{k}}$, $n_{c,\mathbf{k}}$, and $n_{v,\mathbf{k}}$, which constitute the *semiconductor Bloch equations* in Hartree–Fock approximation. For a given electromagnetic light field, these equations may be solved numerically (starting with the unpolarized system before excitation and calculating the temporal evolution).

Let us now look at the interaction between the carriers, i.e., the Coulomb effects. These are marked by the Coulomb potential V_q and occur in the renormalized energies $e_\lambda(\mathbf{k})$ and in a renormalization to the Rabi frequency,

$$\Omega_{\mathrm{Coulomb},\mathbf{k}} = \frac{\left|\mathbf{d}_{cv}\cdot\mathbf{E}(t) + \sum_{\mathbf{q}\neq\mathbf{k}} V_{|\mathbf{k}-\mathbf{q}|} p_{vc,\mathbf{q}}\right|}{\hbar}. \tag{3.59}$$

A characteristic of the Hartree–Fock approximation is thus that Coulomb effects may be represented as renormalization terms.

Neglecting the Coulomb interaction, we regain the *optical Bloch equations*:

$$\left[i\hbar\frac{\mathrm{d}}{\mathrm{d}t} - (\epsilon_c(\mathbf{k}) - \epsilon_v(\mathbf{k}))\right] p_{vc,\mathbf{k}} = [n_{c,\mathbf{k}} - n_{v,\mathbf{k}}]\mathbf{d}_{cv}\cdot\mathbf{E}(t) p_{vc,\mathbf{q}}, \tag{3.60}$$

$$\frac{\mathrm{d}}{\mathrm{d}t} n_{c,\mathbf{k}} = -\frac{\mathrm{d}}{\mathrm{d}t} n_{v,\mathbf{k}} = -\frac{2}{\hbar}\,\mathrm{Im}\left[\mathbf{d}_{cv}\cdot\mathbf{E}(t) p^*_{vc,\mathbf{k}}\right]. \tag{3.61}$$

Here, electrons at different $\mathbf{k}$-values do not couple to each other, i.e., the semiconductor is described as an ensemble of uncoupled two-level systems. Only the Coulomb interaction couples the different wave vectors and makes the semiconductor a true many-body system.

Using the optical Bloch equations and an approach similar to the derivation of Equation 3.36 in Section 3.2 and Equation 3.53, one obtains an often-used formula for the semiconductor absorption or gain [12],

$$\alpha(\hbar\omega) = -g(\hbar\omega) = \frac{\pi e^2}{nc\mathcal{E}_0 m_e^2\omega}|\hat{\mathbf{e}}\cdot\mathbf{d}_{cv}|^2 \int_0^\infty \mathrm{d}E\,\rho_r(E)\frac{\Gamma/(2\pi)}{(E_g + E - \hbar\omega)^2 + (\Gamma/2)^2}\left\{f_v(E) - f_c(E)\right\}, \tag{3.62}$$

$\rho_r(E)$ is the density of states in a three-dimensional parabolic band structure,

$$\rho_r(E) = \frac{1}{2\pi^2}\left(\frac{2m_r}{\hbar^2}\right)^{3/2} E^{1/2}, \tag{3.63}$$

which occurs when transferring from an integral over equally spaced $\mathbf{k}$-values to an energy integral [8,12]. The effective-mass approximation has been used, and m_r is the reduced mass originating from the effective

masses of hole and electron. $\hat{\mathbf{e}}$ is the unit vector pointing in the direction of the light field, and m_e is the free electron mass. The carrier densities n_v, n_c have been replaced by Fermi–Dirac distributions $f_v(E)$, $f_c(E)$, assuming that scattering is fast enough to keep the carrier distributions in thermal equilibrium. This is in general a good approximation especially in a high-density (laser) system; although hole burning or other deviations from an equilibrium distribution may occur [13,14], kinetic holes in the carrier distribution are often smoothed out by the energy integral in Equation 3.62.

Equation 3.62 is thus obtained making, apart from common assumptions such as an infinite crystal lattice, the following approximations:

- Two-band approximation
- Effective-mass approximation, including the assumption of direction-independence of the effective mass
- Neglect of Coulomb interaction between the carriers; many body effects are only included as a phenomenological broadening
- Assumption of a carrier distribution in thermal equilibrium
- Dephasing time $T_2 = 1/\Gamma$ for the decline of the polarization

Looking at laser gain, the spectrum is rather unstructured and deviations between theory and experiment are often compensated by fitting the free parameters of the theory, such as carrier density and broadening; usually, the bandgap is also obtained by fits to experiment. Many gain spectra may thus be fitted with Equation 3.62. A predictive theory, however, needs to take into account many-body effects and closely look at the impact of the other simplifications mentioned above for the structure and experimental conditions it simulates and has to go far beyond the approximations made in Equation 3.62. An excellent overview of the effects of different approximations is given in Ref. [8].

The Hartree–Fock approximation that was introduced above is a widespread method to include many-body effects while keeping computation time reasonable, yet there are many other possible approaches. These include, e.g., (1) the linear case, where the carrier densities are assumed to be zero. The polarization may then be calculated in Hartree–Fock approximation. (2) Calculations beyond Hartree–Fock, where the Coulomb terms are treated in a more elaborate way. In particular, the Coulomb terms also include carrier scattering, which is not mirrored in the Hartree–Fock approximation. Therefore, Hartree–Fock equations require an artificial relaxation to be included. Instead, scattering can be included in the second Born approximation[†] by deriving the equations of motion for four-operator terms and factorizing at this level. This avoids having to include an ad hoc-scattering time, which can only be determined experimentally, and additional changes in temperature, carrier density and other experimental parameters.

Another fact that has not been discussed so far is that realistic semiconductor structures are never perfect. There has been incredible progress in the growth of semiconductor structures since Wolfgang Pauli termed solid-state physics as "dirt physics" in 1931 [15], but there still remain some inhomogeneities and disturbances of the crystal lattice. As was mentioned previously (see Section 3.2.3), disorder introduces a different kind of broadening termed inhomogeneous, where the lineshape is often assumed to be Gaussian.

Thus, different effects are manifest in the lineshape and linewidth of resonances; in other words, the lineshape says a lot about the processes determining it. To illustrate this, Figure 3.3 [16] shows a calculation of a single absorption resonance including homogeneous and inhomogeneous broadening in differing amounts. Both lineshapes include a homogeneous phonon broadening corresponding to a temperature of 30 K; for the calculation of the solid line, an inhomogeneous broadening of 0.287 meV has been added, while for the dotted line only half the disorder strength was included and an additional phenomenological homogeneous broadening of 0.066 meV was introduced via a T_2-time approach. It becomes obvious that homogeneous broadening shifts oscillator strength to the tails of the resonance. In fact, the tails of a Lorentzian lineshape become so strong that unphysical effects may appear, e.g., absorption below the gain resonance of a laser spectrum.

[†] Named after German physicist and mathematician Max Born (1882–1970).

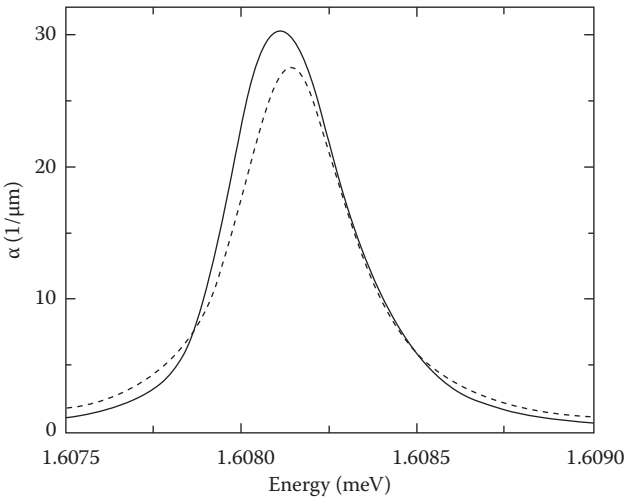

FIGURE 3.3 Absorption of a single resonance for two cases with equal total width, but differing amounts of homogeneous and inhomogeneous broadening. The solid line corresponds to phonon broadening for a temperature of 30 K and disorder broadening of 0.287 meV. For the dashed line, the disorder strength was halved and an additional phenomenological homogeneous broadening of 0.066 meV was introduced. As expected, greater homogeneous broadening results in a more symmetric line shape and stronger tails. (From A. Thränhardt et al., *Phys. Rev. B.*, 68, 035316, 2003.)

3.4 Quantization of the Light Field

Thus far, we have worked with semiclassical descriptions, i.e., including a classical light field. Yet it was shown in Section 3.2.1 that any system requires a spontaneous emission term even in a simple model, whereas in Section 3.2.2 it became apparent that the semiclassical model does not offer a term to that extent. Looking at the device aspect, we remark that the simplest optoelectronic device, the LED, emits light entirely due to spontaneous emission, and the laser diode depends on it for start-up. Quantum effects also play a role, e.g., in nanolasers and single quantum dots in resonators [17]. We thus briefly discuss quantization of the electromagnetic field. Due to the rich range of phenomena involved we leave the major discussion to the wealth of textbooks on the market, e.g., Refs. [18,19] among many others.

Consider again a two-level atom. The Hamiltonian of the fully quantized system consists of three parts,

$$\hat{H} = \hat{H}_{\text{atom}} + \hat{H}_{\text{light}} + \hat{H}_{\text{int}}\,, \tag{3.64}$$

where $\hat{H}_{\text{atom}}$ corresponds to the Hamiltonian of the undisturbed electron system (formerly $\hat{H}_0$), $\hat{H}_{\text{light}}$ is the Hamiltonian of the undisturbed light system, and $\hat{H}_{\text{int}}$ describes the interaction between the two.

Looking at a system in free space, we need to take into account a variety of photon modes characterized by their wave vectors $\mathbf{q}$ pointing in all directions. Spontaneous emission of a two-level atom can then be calculated. Starting from the excited two-level atom, the system wave function can be written as

$$|\Psi(t)\rangle = \hat{a}(t)e^{-i\omega_0 t}|e;0\rangle + \sum_{\mathbf{q},s} \hat{b}_{\mathbf{q},s}(t)e^{-i\omega_q t}|g;1_{\mathbf{q},s}\rangle\,, \tag{3.65}$$

i.e., either the system is in its initial state $|e;0\rangle$ where the atom is excited and there is no photon, or a photon with wave vector $\mathbf{q}$ and polarization s has been emitted and the atom thus returned to its ground state, yielding a wave vector $|g;1_{\mathbf{q},s}\rangle$. Here, the energy of the photon will correspond to the energy difference of the two-level system $\hbar\omega_0$, thus the absolute value of the photon wave vector $q = \omega_0/c$ is well defined, but

not its direction. In 1930, Weisskopf[†] and Wigner[‡] found an irreversible exponential decay of the atom with a decay rate equal to Einstein's A coefficient (see Equation 3.11) [20].

We briefly discuss another case here, where there is only one photon mode at the energy $\hbar\omega_C$. Consider, e.g., a two-level atom in a cavity only allowing a specific photon mode, leading us to the Jaynes–Cummings model [21]. The undisturbed photon Hamiltonian is

$$\hat{H}_{\text{light}} = \hbar\omega_C \hat{a}^\dagger \hat{a}\,. \tag{3.66}$$

Here, $\hat{a}^\dagger$ ($\hat{a}$) is a photon creation (annihilation) operator. The atom Hamiltonian remains unchanged,

$$\hat{H}_{\text{atom}} = \epsilon_1 |1\rangle\langle 1| + \epsilon_2 |2\rangle\langle 2| = \hbar\omega_0 |2\rangle\langle 2|, \tag{3.67}$$

by setting $\epsilon_1 = 0$ and $\epsilon_2 = \hbar\omega_0$. We introduce the ladder operators

$$\begin{aligned} \hat{\sigma}^+ &= |2\rangle\langle 1|, \\ \hat{\sigma}^- &= |1\rangle\langle 2|, \end{aligned} \tag{3.68}$$

expressing the transfer of the electron from level 1 to level 2 and vice versa, respectively. Next, we rewrite $\hat{H}_{\text{atom}}$ as

$$\hat{H}_{\text{atom}} = \hbar\omega_0 \hat{\sigma}^+ \hat{\sigma}^- \tag{3.69}$$

and express the interaction Hamiltonian in RWA as

$$\hat{H}_{\text{int}} = \hbar g(\hat{a}^\dagger \hat{\sigma}^- + \hat{a}\hat{\sigma}^+), \tag{3.70}$$

where g is the coupling strength. The RWA expresses that, whenever a photon is created, the electron has to drop from the excited state to the ground state ($\hat{a}^\dagger\hat{\sigma}^-$) and when a photon is absorbed, the electron has to jump from the ground state into the excited state ($\hat{a}\hat{\sigma}^+$).

The Jaynes–Cummings Hamiltonian may then be solved by writing it in a matrix representation and diagonalizing this matrix. Looking at Equation 3.65, the wave functions must be linear combinations of $|2, n\rangle$ (the atom is in the excited state, state 2, and there are n photons in the system) and state $|1, n+1\rangle$ (the atom is in the ground state, state 1, and there are $n+1$ photons in the system). However, $|2, n\rangle$ and $|1, n+1\rangle$ are not the eigenstates of the system any more. They are often called the bare states while the true eigenstates, which result from diagonalization of Hamiltonian (3.64), are referred to as dressed states. On resonance, they are found to be

$$\begin{aligned} |S\rangle &= \frac{|2, n\rangle + |1, n+1\rangle}{\sqrt{2}}, \\ |A\rangle &= \frac{|2, n\rangle - |1, n+1\rangle}{\sqrt{2}}. \end{aligned} \tag{3.71}$$

Similar to the semiclassical case, for a system initially in the upper state this results in an oscillation:

$$\begin{aligned} |c_{en}(t)|^2 &= \cos^2\left(g\sqrt{n+1}t\right), \\ |c_{gn+1}(t)|^2 &= \sin^2\left(g\sqrt{n+1}t\right). \end{aligned} \tag{3.72}$$

[†] Victor Frederick Weisskopf, Austrian-born American physicist (1908–2002).
[‡] Eugene Paul Wigner, Hungarian-American physicist (1902–1995).

There is, however, an important difference for the case $n = 0$, i.e., when no light field is present: While from Equation (3.20), we obtain $\Omega = 0$ for the semiclassical case (i.e., no Rabi oscillations occur), the quantum optical calculation yields the so-called vacuum Rabi oscillations with nonzero vacuum Rabi frequency. The excited atom periodically emits and reabsorbs a photon.

An interesting case also occurs if the two-level system interacts not with a single photon state $|n\rangle$, but with a coherent superposition of photon states. In this case, the probability of finding the system in the excited state will dephase due to the different Rabi frequencies of the various photon states; however, at certain times there will be a revival of the excited state because of constructive interference. This "quantum revival" was predicted theoretically in 1980 [22] and experimentally observed in 1987 [23].

3.5 Role of the Electromagnetic Environment

Thus far, we have not considered the structure of the photon wave function at all. However, for the Jaynes–Cummings model (see Section 3.4), we consider the interaction of a two-level system with a single photon mode. For the preparation of this system, a high-quality microcavity is required. As we have seen, the strength of the light field at the location of the electron determines the interaction strength between light and matter. Therefore, resonators are widely used to engineer electron–photon interaction processes, and the last section deals with the theoretical handling of these structures.

In resonator structures, calculation of the appropriate photon modes is required to allow access to the strength of electron–photon coupling. This will be clarified using the example of a microcavity. Modes can be established by a transfer-matrix method, which will be briefly discussed. For simplicity, we only look at a planar structure and perpendicular light incidence in this book chapter, while for in-depth information, the reader is referred to Refs. [24,25]. Information on the transfer matrix method may also be found in Ref. [26] and the references therein.

In free space or homogeneous matter, plane waves $\mathbf{E}_0 e^{i(\mathbf{q}\cdot\mathbf{r}-\omega t)}$ are solutions to Maxwell's equations [4]. Any light field may be expanded in plane waves. The transfer matrix method uses this to express the light field as a plane wave in every layer of a microstructure and appropriately match the conditions at the interfaces.

We consider a planar structure where the growth direction is taken as the z-axis. The index of refraction then only depends on z. The homogeneous wave equation reads

$$\left\{ \frac{1}{c^2}\frac{\partial}{\partial t^2} - \Delta \right\} \mathbf{u}_\mathbf{q}(z) = 0\,, \tag{3.73}$$

where $\mathbf{u}_\mathbf{q}(z)$ is the light mode we are looking for, indexed with its wave vector $\mathbf{q}$. Since we are looking at perpendicular incidence in a planar structure, the wave vector points in the z-direction. Due to the geometry of the problem, the two independent polarizations are equivalent to each other. The index of polarization is thus omitted here, and bearing in mind that we need to find two independent modes for each wave vector q. The polarization becomes important for incidence at an angle.

Consider first a single boundary between two layers L (left) and R (right). Generally, each mode $\mathbf{u}_\mathbf{q}(z)$ is a combination of plane waves traveling in forward and backward directions in each layer,

$$\begin{aligned} \mathbf{u}_\mathbf{q}(z) &= A_j e^{iq_{zj}(z-z_j)}\mathbf{e}_j + B_j e^{-iq_{zj}(z-z_j)}\mathbf{e}'_j \\ \text{where} \quad q_{zj} &= n(z_j)\,q\,. \end{aligned} \tag{3.74}$$

Maxwell's equations demand continuity for the tangential components of the electric and magnetic field and thus (in this geometry) for the entire mode $\mathbf{u}_\mathbf{q}(z)$ and its derivation $\mathrm{d}/\mathrm{d}z\mathbf{u}_\mathbf{q}(z)$. From this condition,

transmission and reflection may be derived as

$$T_j^- = \frac{2q_{z,j}}{q_{z,j} + q_{z,j+1}}, \tag{3.75}$$

$$R_j^- = \frac{q_{z,j} - q_{z,j+1}}{q_{z,j} + q_{z,j+1}}, \tag{3.76}$$

$$T_j^+ = \frac{2q_{z,j+1}}{q_{z,j} + q_{z,j+1}}, \tag{3.77}$$

$$R_j^+ = \frac{q_{z,j+1} - q_{z,j}}{q_{z,j} + q_{z,j+1}}; \tag{3.78}$$

see Ref. [4] for more details. T_j^- and R_j^- (T_j^+ and R_j^+) are transmission and reflection coefficients for light incident from the left (right) side, respectively. This may be generalized to a matrix representation, relating neighboring heterostructure layers by

$$\begin{pmatrix} A_{j+1} \\ B_{j+1} \end{pmatrix} = \frac{1}{T_j^+} \begin{pmatrix} e^{iq_{z,j}d_j} & R_j^+ e^{-iq_{z,j}d_j} \\ -R_j^- e^{iq_{z,j}d_j} & e^{-iq_{z,j}d_j} \end{pmatrix} \begin{pmatrix} A_j \\ B_j \end{pmatrix} \equiv \mathbf{M}_j \begin{pmatrix} A_j \\ B_j \end{pmatrix}, \tag{3.79}$$

where d_j is the width of layer j, $d_j = z_j - z_{j+1}$, and $\mathbf{M}_j$ is the transfer matrix. Recursive application yields

$$\begin{pmatrix} A_{N+1} \\ B_{N+1} \end{pmatrix} = \mathbf{M}_N \mathbf{M}_{N-1} \ldots \mathbf{M}_2 \mathbf{M}_1 \begin{pmatrix} A_1 \\ B_1 \end{pmatrix} \equiv \mathbf{M}_{tot} \begin{pmatrix} A_1 \\ B_1 \end{pmatrix} \tag{3.80}$$

and allows the calculation of modes $\mathbf{u}_\mathbf{q}^+(z)$ and $\mathbf{u}_\mathbf{q}^-(z)$ incident from the left and right of the microcavity. Figure 3.4 [27]. shows a resonant mode in a typical Galliumarsenide (GaAs)/Aluminiumarsenide (AlAs) microcavity structure with 10 layer pairs on top and 20 layer pairs on the substrate. It becomes obvious that

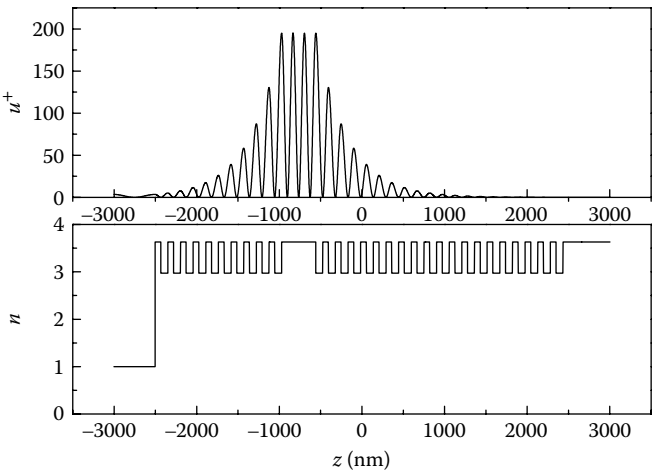

FIGURE 3.4 Top: Central mode of a GaAs/AlAs microcavity with 10 (on air) and 20 (on substrate) λ/4 layer pairs of GaAs and AlAs with background refractive indices of $n_{\mathrm{GaAs}} = 3.63$ and $n_{\mathrm{AlAs}} = 2.97$, respectively. Bottom: Refractive index of the microcavity along the growth direction z. (From A. Thränhardt, Equilibrium and Nonequilibrium Dynamics in Semiconductor Lasers, Habilitation Thesis, Marburg, 2006.)

the electric light field is enhanced by a factor of about 200 even in this simple structure in the peaks in the cavity. In this way, light–matter interaction may be reinforced by several orders of magnitude. Of course, photonic engineering also works for two- or three-dimensional photonic crystal structures where more elaborate theoretical approaches have to be used for the calculation of the modes, e.g., the finite difference time domain (FDTD) method [28,29], where electric and magnetic field components are calculated alternately.

References

1. P. A. M. Dirac, The quantum theory of the emission and absorption of radiation, *Proc. R. Soc. A* **114**, 243 (1927).
2. L. Allen, J. H. Eberly, *Optical Resonance and Two-Level Atoms, Dover Books on Physics*, New York, (1988) (revised edition).
3. A. Einstein, Zur Quantentheorie der Strahlung, *Phys. Zeitschrift* **18**, 121 (1917), first published in *Mitteilungen der Phys. Ges. Zürich* 18 (1916).
4. J. D. Jackson, *Classical Electrodynamics*, 3rd ed., New York: Wiley (1999).
5. J. Mompart, R. Corbalán, Lasing without inversion, *J. Opt. B: Quantum Semiclass. Opt*. **2**, R7 (2000).
6. M. D. Frogley, J. F. Dynes, M. Beck, J. Faist, C. C. Phillips, Gain without inversion in semiconductor nanostructures, *Nat. Mater.* **5**, 175 (2006).
7. H. Haug, S. W. Koch, *Quantum Theory of the Optical and Electronic Properties of Semiconductors*, 5th ed., Singapore: World Scientific (2009).
8. W. W. Chow, S. W. Koch, *Semiconductor–Laser Fundamentals*, Berlin/Heidelberg: Springer (1999).
9. S. Adachi, *GaAs and Related Materials: Bulk Semiconducting and Superlattice Properties*, Singapore: World Scientific (1994).
10. G. Franco Bassani, G. Pastori Parravicini, *Electronic States and Optical Transitions in Solids*, New York, NY: Pergamon Press (1975).
11. D. Dragoman, M. Dragoman, *Optical Characterization of Solids*, Berlin/Heidelberg: Springer (2010).
12. Shun Lien Chuang, *Physics of Optoelectronic Devices*, New York/Brisbane/Singapore: Wiley-InterScience (1995).
13. A. Thränhardt, S. Becker, C. Schlichenmaier, I. Kuznetsova, T. Meier, S. W. Koch, J. Hader, J. V. Moloney, W. W. Chow, Nonequilibrium gain in optically pumped GaInNAs laser structures, *Appl. Phys. Lett*. **85**, 5526 (2004).
14. E. Kühn, S. W. Koch, A. Thränhardt, J. Hader, J. V. Moloney, Microscopic simulation of nonequilibrium features in quantum-well pumped semiconductor disk lasers, *Appl. Phys. Lett*. **96**, 051116 (2010).
15. K. V. Meyenn (Ed.), *Wolfgang Pauli: Wissenschaftlicher Briefwechsel mit Bohr, Einstein, Heisenberg u.a. Band II: 1930–1939/Scientific Correspondence with Bohr, Einstein, Heisenberg a.o.*, Berlin/Heidelberg/New York, NY/Tokyo: Springer, Reprint (2014).
16. A. Thränhardt, C. Ell, S. Mosor, G. Rupper, G. Khitrova, H. M. Gibbs, S. W. Koch, Interplay of phonon and disorder scattering in semiconductor quantum wells, *Phys. Rev. B* **68**, 035316, 2003.
17. F. Jahnke (ed.), *Quantum Optics with Semiconductor Nanostructures*, Oxford/Cambridge/Philadelphia/New Delhi: Woodhead Publishing Series in Electronic and Optical Materials (2012).
18. P. Meystre, M. Sargent III, *Elements of Quantum Optics*, 4th ed., Berlin/Heidelberg: Springer (2010).
19. M. Kira, S. W. Koch, *Semiconductor Quantum Optics*, Cambridge: Cambridge University Press (2011).
20. V. Weisskopf, E. Wigner, Berechnung der natürlichen Linienbreite auf Grund der Diracschen Lichttheorie, *Zeitschrift für Physik* **63**, 54 (1930).
21. E. T. Jaynes, F. W. Cummings, Comparison of quantum and semiclassical radiation theories with application to the beam maser, *Proc. IEEE* **51**, 89 (1963).

22. J. H. Eberly, N. B. Narozhny, J. J. Sanchez-Mondragon, Periodic spontaneous collapse and revival in a simple quantum model, *Phys. Rev. Lett*. **44**, 1323 (1980).
23. G. Rempe, H. Walther, N. Klein, Observation of quantum collapse and revival in a one-atom MASER, *Phys. Rev. Lett*. **58**, 353 (1987).
24. M. Born, E. Wolf, *Principles of Optics: Electromagnetic Theory of Propagation, Interference and Diffraction of Light*, 7th ed., Cambridge: Cambridge University Press (2002).
25. B. E. Sernelius, *Surface Modes in Physics*, Berlin: Wiley-VCH (2001).
26. G. Khitrova, H. M. Gibbs, F. Jahnke, M. Kira, S. W. Koch, Nonlinear optics of normal-mode-coupling semiconductor microcavities, *Rev. Mod. Phys*. **71** (5), 1591 (1999).
27. A. Thränhardt, Equilibrium and Nonequilibrium Dynamics in Semiconductor Lasers, Habilitation Thesis, Marburg (2006).
28. K. Yee, Numerical solution of initial boundary value problems involving Maxwell's equations in isotropic media, *IEEE Trans. Antennas. Propag.* **14**, 302 (1966).
29. D. M. Sullivan, *Electromagnetic Simulation Using the FDTD Method*, Hoboken/New Jersey: Wiley, 2013.